DEVELOPMENT, TESTING, PERFORMANCE ANALYSIS AND MODELLING OF A BIOCHAR-BASED CATALYST FOR METHANATION REACTION

Begoña Peña[a]*, Manuel Bailera[a], Jorge Legaz[a], Cristian Barón[a], Silvia Garlatti[b], Elena Martín[c], M. Zampilli[b], K. L. Slopiecka[b], Jordi Guilera[c], Francesco Fantozzi[b], Luis M. Romeo[a], Pilar Lisbona[a]

[a] Energy and CO_2 Group, Aragon Institute of Engineering Research (I3A), Department of Mechanical Engineering, Escuela de Ingeniería y Arquitectura, Universidad de Zaragoza, María de Luna 3, 50018 Zaragoza, Spain.
[b] SESLAB, University of Perugia, Italy
[c] Catalonia Energy Research Institute (IREC), Spain

*Corresponding Author: bpp@unizar.es

ABSTRACT

Hydrogenation of carbon dioxide to produce synthetic methane is a promising alternative to reduce the dependence on fossil fuels of high-temperature industrial processes hard to be electrified, contributing to mitigation of global warming. To reach enough conversion ratios and reasonable reactor sizes, the Sabatier reaction, in which the process is based, is usually performed via heterogeneous catalysis. Metallic catalysts, as nickel (Ni) or ruthenium (Ru) that exhibit high stability for long operation times and resistance to sintering and carbon deposition, are the most used, supported over mesoporous alumina. The present work proposes and analyses the use of biochar obtained from olive kernel pyrolyzed at 600 °C for 2 h and successively activated by steam at 750 °C for 1 h. The so-obtained biochar, with a specific surface area of 320 m^2/g, is then evaluated as a cost-effective and sustainable support for methanation catalysts. A Ni-based (10 % wt.) catalyst was developed and tested in a fixed-bed methanation pilot plant. The obtained conversion ratios for GHSV (gas hourly space velocity) of 6000 h^{-1} were above 80% and 95% for H_2:CO_2 ratios of 4 (stoichiometric condition) and 5.5, respectively. Furthermore, a kinetic model was developed and validated with the experimental measurements, founding low minimum mean squared error between the kinetic model and the experiment. The kinetic model was implemented in Aspen Plus to potentially be used in integrated application models based in power to gas concepts. Additionally, N_2-physisorption and H_2-TPR analyses have served to characterize the fresh and used samples of the Ni-biochar catalyst.

1 INTRODUCTION

The most efficient and selective catalysts studied for methanation purposes are noble metals like Rh (Petersen et al., 2021) and Pt (Younas et al., 2018), although their high cost and limited availability has shifted the research studies toward more feasible alternatives, such as transition metal-based catalysts (Renda et al., 2021). Heterogeneous catalysts are composed of metals belonging to the VIII-XI groups, among which the most used are Ni and Ru due to their competitiveness in terms of efficiency in methane yield and production cost.

The catalysts need to be supported on a carrier material which is as more efficient as more active metallic phase is able to adsorb. One of the main feature that a carrier should have is therefore a large specific surface area, but it should preferably be at the same time cheap and sustainable (Mei et al., 2023). The most used commercial carriers are Al_2O_3, SiO_2, ZrO_2, CeO_2, zeolite and other mesoporous structural supports (Paviotti et al., 2021).

https://doi.org/10.52202/077185-0199

Lately low-cost carbon-based supports like activated carbon and carbon nanotubes are gaining interest thanks to their chemical stability and surface chemical reactivity (Cam et al., 2019) (Feng et al., 2016)(Wang et al., 2014)(Wang et al., 2019)(Antoniak-Jurak et al., 2015)(Antoniak-Jurak et al., 2016). Carbon materials such as activated carbon or biochar are indeed characterized by a high ability of Ni recovering by combustion after the use of char-supported catalysts that cannot be made with conventional support materials (Mei et al., 2023)(Swalus et al., 2012)(Yue et al., 2021)(Luo et al., 2021). Biochar is an aromatic carbon-rich solid generated via thermochemical processes from biomass under oxygen-free or oxygen-limited conditions (Avagyan, 2020)(Manyà, 2012), which compared to other carbon supports is cheap and versatile (Wang et al., 2014). It can be produced from a wide range of waste materials, which encompass wood or crop residues, as well as livestock and food processing waste (Avagyan, 2020). The physicochemical properties of biochar are significantly influenced by the temperature, heating rate and holding time at which it is produced (Dudek et al., 2019). Such a kind of scaffold offers the chance to lower the price of catalysts and at the same time enhance circular economy by pyrolyzing a waste or a by-product to obtain char instead of buying raw materials such as Al_2O_3.

Physical activation involves the use of a gaseous activating agent, usually steam or CO_2 which are delivered to the solid material once the pyrolysis process has ended. Generally activation takes place at a temperature between 700°C and 1000°C. During this process the carbon atoms with a higher reactivity are removed in the form of CO, leading to an increase in the porosity and surface area of the solid material.

The drawback of biochar and activated carbon production is usually related to a high energy consumption and the elevated microporosity of their structure can be a limitation for the diffusion of reactants and products, which occurs more likely in the presence of mesopores that are usually formed during the activation processes of carbon as consequence of collapses in the porous structure (Di Stasi et al., 2021)(Kumar and Sinha, 2020). In addition, reactive matrixes such as biochar are often susceptible to mass loss of the support and modifications of catalyst behaviour caused by the gasification reaction occurring on char, which is favoured by the heat released during methanation and leads to the formation of structural defects on the carrier and to the destruction of the existing Ni-C bondages (Wang et al., 2014)(Mei et al., 2023). This phenomenon considerably reduces the service of life of the catalyst and is the main parameter that needs to be refined by further studies.

This work tackles the assessment of a biochar-nickel based catalyst for the methanation reaction. A complete study is presented, including the production of biochar support, the preparation and characterization of the samples, the testing in a pilot-scale reactor and a kinetic model adjusted with the experimental data.

2 METHODOLOGY

2.1 Biochar production process

The catalyst support in the present work consists of activated biochar particles of ≤1 mm diameter. The starting biomass employed for biochar production is a largely available olive milling waste, namely olive kernel, which is pyrolyzed and physically activated using steam at 750 °C. The details of the preparation of the material are presented below.

2.1.1.Biochar production: The olive kernel biochar was obtained through batch pyrolysis conducted at Seslab (Sustainable Energy systems Laboratory) - Department of Engineering, University of Perugia. The pyrolysis batch reactor is a stainless steel cylindrical bin with an internal diameter of 15 cm and a height of 30 cm, heated with an electric heater composed of two semi-cylindrical ceramic shells (Figure 1).

https://doi.org/10.52202/077185-0199

After previous inertization, made by blowing into the reactor N_2 at a flow rate of 200 mL/min, the process was started at room temperature reaching the set point with a heating rate of 5-10 °C/min. For each biomass the pyrolysis test was carried out at two temperature set points, namely 400 °C and 600 °C. The total retention time was 2 hours, after which the system was allowed to cool down to room temperature. The char remained inside the reactor was weighed and stored before being characterized and employed in the activation trials.

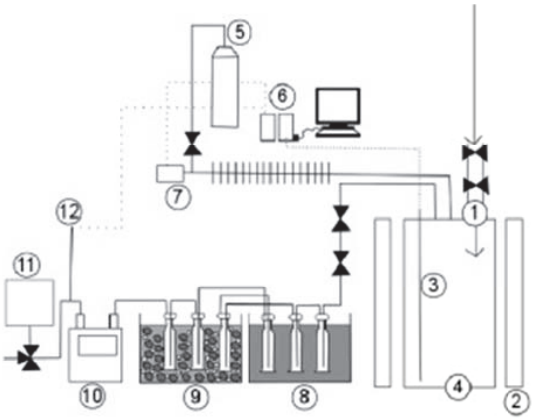

Figure 1: Pyrolysis facility. (1) biomass inlet, (2) electrical heaters, (3) thermocouple, (4) reactor, (5) inert gas bottle (N_2), (6) data acquisition system, (7) pressure sensor, (8) warm bath with impingers, (9) cold bath with impingers, (10) flowmeter, (11) sampling bag, (12) thermocouple to gas outlet

2.1.2. Biochar activation: Steam activation was performed in a vertical tubular reactor by injecting water at 2 mL/g h^{-1} for 1 hour. The reactor consisted in a cylindrical tube with an internal diameter of 39 mm and a height of 420 mm. The water inlet was located at the top of the reactor and was provided with a valve that was opened to inject water by means of a syringe and immediately closed to avoid the entrance of oxygen. The steam formed by the water once reached 100 °C was successively carried into the reactor through a tube connected to the water inlet, long 370 mm. The distance between the end of the tube and the bottom of the reactor measured about 4 cm and was assumed to be not completely reached by steam. This made it necessary to create a quartz and char bed high approximately 5 cm with the aim of supporting the sample to be activated while leading steam to flow from the inlet tube to the upper part of the reactor. The sample was collocated right above the steam exit and was in turn covered with another layer of filtering char and quartz gravel. At 360 mm from the top of the reactor was located the outlet tube of steam, being this point the higher part of the facility reached by the mix of char and quartz.

Biochar was minced in a mortar to produce char with a particle size of about 1 mm. The reactor was charged with a layer of quartz gravel until a height of 5 cm was reached. Above this support bed 30 g of biochar were inserted into the reactor and subsequently topped with about the same amount of quartz gravel placed to the bottom. 200 mL of water were prepared to charge 5 mL syringes, which were calculated to be emptied approximately every 2 minutes in order to achieve a total of 100 mL of water delivered per hour. For each biochar typology the activation was carried out during 1 and 2 hours. The reactor was pre-heated with a ramp of 10 °C/min until 750 °C were reached, successively the water injection was started and, after the selected activation time was over, the reactor was gradually cooled down to room temperature before being opened to collect the activated char. Afterwards, the biochar was separated from the quartz gravel using a 2 mm sized sieve and stored before catalyst preparation.

https://doi.org/10.52202/077185-0199

2.2 Biochar-based catalyst preparation

For the synthesis of the supported Ni catalyst, 33 g of nickel nitrate hexahydrate ($Ni(NO_3)_2 \cdot 6H_2O$) were dissolved in 72 mL of deionized water. Subsequently, 60 g of biochar were introduced into the solution, and the resulting mixture underwent agitation for 1 hour to facilitate homogenous distribution. Following dissolution, the solvent was removed through vacuum-assisted evaporation utilizing a rotary evaporator set at 80°C during 4 hours.

The resultant solid product underwent desiccation at 105°C for 12 hours to ensure complete elimination of residual moisture. The dried material was calcined at 450°C, employing a heating rate of 1°C per minute over a period of 30 minutes.

2.3 Experimental facility and planning

The methanation experiments were performed in a fixed-bed reactor integrated in the facility shown in Figure 2. It includes a ceramic preheater to increase the temperature of the H_2/CO_2 mixture fed from bottles up to 225-245 °C. Two mass flow controllers allow regulating the Gas Hourly Space Velocity (GHSV, Eq.(1)) and the H_2/CO_2 molar ratio. The gas composition is measured at the inlet and the outlet of the reactor with a gas analyser for H_2, CO_2, CO and CH_4. After the methanation stage, the water produced is condensed before the measurement of the final gas composition with the gas analyser. The outlet gas mixture is finally burnt. For cleaning and heating purposes, the facility also includes a N_2 entry before the electrical heater.

$$GHSV = \frac{F}{m_{cat}/\rho_{cat}} \quad (1)$$

In the fixed-bed reactor with a double-pipe design of parallel flows (Figure 3), reactants flow downward inside the inner tube (620 mm length and 30 mm inner diameter) undergoing the heterogeneous methanation reaction getting in contact with the solid catalyst. The heat released in this exothermic reaction may be removed through the injection of a parallel cooling air flow in the outer tube (outer diameter of 100 mm) to control the temperature of the reactor, avoiding the formation of hot spots. The heating up of the reactor during the start-up of the facility is achieved with electrical resistances of 900 W, installed around the double-pipe reactor.

A total of nine K-type thermocouples (T1-T9) are uniformly distributed along the reactor length (50 mm of separation). These are in contact with the wall of the inner tube to indirectly measure the temperature of the fixed bed. In addition, a multipoint thermocouple probe measures the temperature in five points of the fixed-bed axis (L5-L1), being located at the same level of thermocouples T2-T6 for comparison purposes.

https://doi.org/10.52202/077185-0199

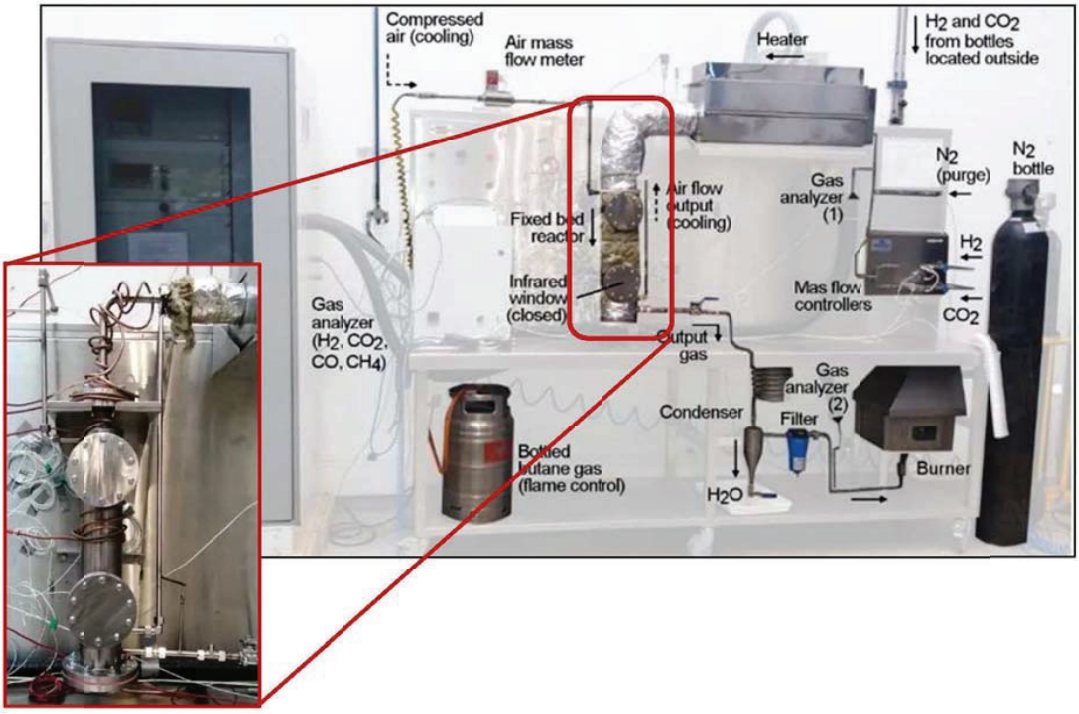

Figure 2: Methanation test facility (left) and detail of the double-pipe reactor without isolation

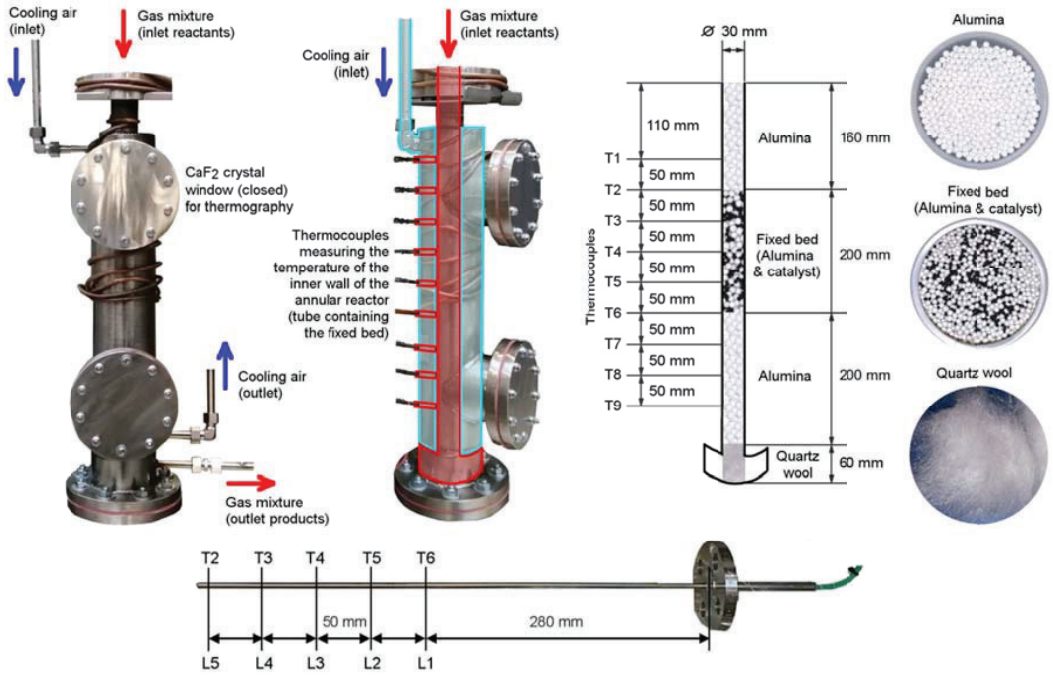

Figure 3: Detail of the fixed-bed reactor and the location of thermocouples

https://doi.org/10.52202/077185-0199

Each experiment includes three stages: pre-heating, activation and methanation. In the pre-heating stage, N_2 previously heated up in the ceramic furnace is passed through the fixed bed reactor. Additionally, the electrical resistances preheat the reactor from the outside. When the average temperature of the reactor reaches 250 ºC, the catalyst activation is performed during 60 min. During the activation stage, a mass flow of 20 g/h of pre-heated pure H_2 is continuously fed to the reactor. After pre-heating and activation stages, the electrical resistances are turned off and different stationary states are searched. Methanation tests start with the injection of reactants at proper conditions to reach constant carbon conversion and temperatures, paying special attention to the region of the reactor where methanation reaction is more intense. The timeframe established to achieve each stationary state is 5-6 min. Carbon conversion (Eq. (2)) and selectivity to methane (Eq. (3)) are easily calculated through the inlet flows and the information provided by the gas analyser before and after methanation stage. Specifically, $\dot{n}_{i,0}$ is the mole flow of component i at the inlet, and $\dot{n}_i$ at the outlet.

Table ***1*** summarizes the ranges in which the operating parameters vary during the experiments

$$x_{CO2} = \frac{\dot{n}_{CO2,0} - \dot{n}_{CO2}}{\dot{n}_{CO2,0}} 100 \quad (2)$$

$$s_{CH4} = \frac{\dot{n}_{CH4}}{\dot{n}_{CH4} + \dot{n}_{CO}} 100 \quad (3)$$

Table 1: Parameters varied in the experimental tests

Parameter	Minimum	Maximum
Temperature (ºC)	200	500
H_2/CO_2	3.5	5.5
GHSV (h^{-1})	2000	80000
Catalyst mass (g)	5	40

2.4 Kinetic model development

A kinetic model was developed for the Ni-biochar catalyst, considering the two main reactions (eq. (4) and. (5)):

$$CO + H_2O \leftrightarrow CO_2 + H_2 \quad (4)$$

$$CH_4 + H_2O \leftrightarrow CO + 3H_2 \quad (5)$$

The reaction rates follow Eq.(6) and (7), respectively, according to the model proposed by Xu and Froment (Xu and Froment, 1989).

$$r_1 = \frac{\frac{k_1}{p_{H2}}\left(p_{CO}p_{H2O} - \frac{p_{CO2}p_{H2}}{K_{eq1}}\right)}{\left(1 + K_{CO}p_{CO} + K_{H2}p_{H2} + K_{CH4}p_{CH4} + \frac{K_{H2O}p_{H2O}}{p_{H2}}\right)^2} \quad (6)$$

$$r_2 = \frac{\frac{k_2}{p_{H2}^{2.5}}\left(p_{CH4}p_{H2O} - \frac{p_{CO}p_{H2}^3}{K_{eq2}}\right)}{\left(1 + K_{CO}p_{CO} + K_{H2}p_{H2} + K_{CH4}p_{CH4} + \frac{K_{H2O}p_{H2O}}{p_{H2}}\right)^2} \quad (7)$$

where p_i are the partial pressures of the components, k_i is the rate coefficient (Eq.(8), Arrhenius equation), K_{eq} is the equilibrium constant (Eq.(9)-(10)), and K_i are the adsorption constants of each component (Eq.(11)).

https://doi.org/10.52202/077185-0199

$$k_i = k_{i,0} \cdot \exp\left(-\frac{E_{A,i}}{R \cdot T}\right) \tag{8}$$

$$K_{eq1} = \exp\left(\frac{4400}{T} - 4.063\right) \tag{9}$$

$$K_{eq2} = 1.026676 \times 10^{10} \exp\left(\frac{-26830}{T} + 30.11\right) \tag{10}$$

$$K_i = K_{i,0} \cdot \exp\left(-\frac{\Delta H_i^0}{R \cdot T}\right) \tag{11}$$

The parameters $k_{i,0}$ (pre-exponential factor), $E_{A,i}$ (activation energy) and $K_{i,0}$ (adsorption constants were obtained by minimizing the arithmetic mean of the mean squared error (MSE) for the CO_2 conversion (Eq.(2) and for the CH_4 selectivity (Eq (3)). The M_{MSE} was minimized by using the Powell Method (Vassiliadis and Conejeros, 2008). Half of the experimental data was used for adjusting the kinetic model, and the other half was used for validating the model.

3 RESULTS AND DISCUSSION

3.1 Methanation results

Preliminary experimental tests were performed in the methanation facility described above (Figure 2 and Figure 3) with two fixed-beds containing 5 and 40 g of Ni-biochar catalyst. The preliminary results are gathered in Figure 4, where CO_2 conversion and CH_4 selectivity are represented under different operation conditions. The expected trends are obtained. Conversion increases rapidly above 250 ºC, being faster for 40 g of catalyst. When H_2/CO_2 ratio is varied from 3.5 to 5.5, conversion augments. Temperature is kept around 350ºC for 5 g, while is about 475 ºC for 40 g. Conversion drops as GHSV increases, under stoichiometric molar ratio. High GHSV has been reached with 5 g of catalyst in order to obtain conditions of low CO_2 conversion rates.

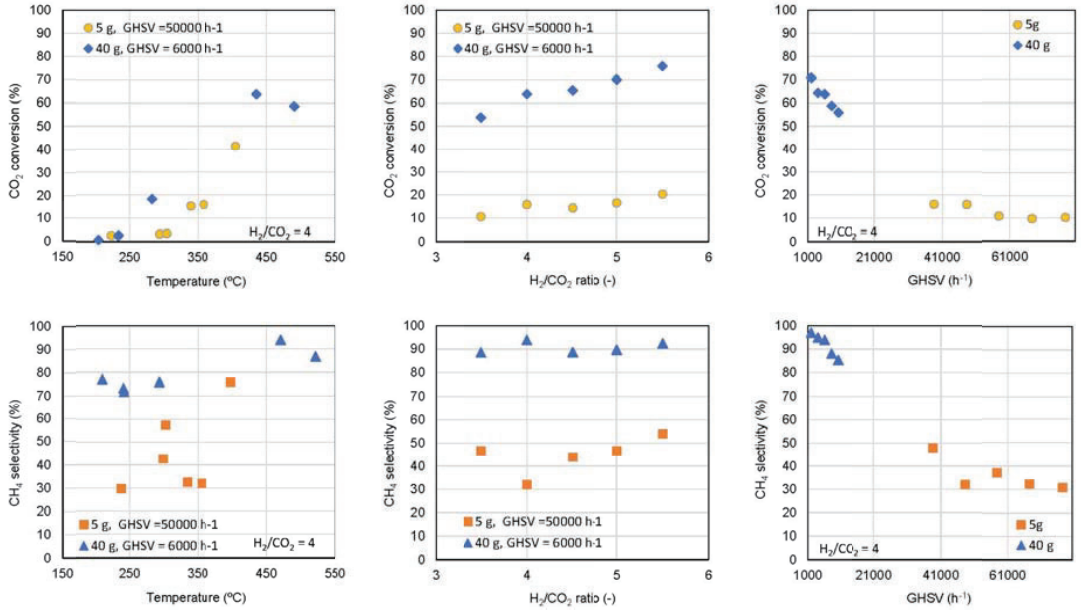

Figure 4: Carbon conversion and selectivity to methane under different operation conditions

https://doi.org/10.52202/077185-0199

Regarding selectivity to methane, the dependency with temperature is unclear. For the tests with 40 g, an increasing trend is observed. Nevertheless, further experiments are needed to be clarified. As for the molar ratio, a slightly positive effect is observed for 5 g, but selectivity keeps quite constant around 90% for 40 g. Finally, the increase of GHSV results in decreasing selectivity.

3.2 Sample characterization

The textural properties of the steam-activated biochar and the Ni/biochar catalyst were studied by N_2-physisorption (see Table 2). The bare biochar support exhibited an initial surface area (SABET) of 530.6 m^2/g. Subsequent to Ni deposition, a decrease in surface area was observed, indicating effective occupation of biochar pores by Ni particles. Despite the decrease in surface area, the resulting catalyst preserved a significant surface of 500.7 m^2/g—an essential feature for achieving optimal catalytic activity.

Table 2: Sample characterization

	SA_{BET} (m^2/g)	Pore volumen (cm^3/g)	Pore size (nm)
Sa-biochar	530.6	0.25	4.9
Ni/sa-biochar	500.7	0.26	5.1

The reducibility of the synthetized Ni/biochar catalyst was examined by H_2-TPR (Figure 5). A distinct reduction peak observed at temperatures below 400 ºC suggests NiO bulk weakly interacting with the support. In contrast, Ni species reduced at temperatures beyond 400 ºC indicate moderate to strong interactions with the biochar surface. It's noteworthy that, at a reduction temperature of 400ºC, the catalyst does not undergo complete reduction to its active metallic phase. This observation is evident in the H_2-TPR profile of the used catalyst, where NiO species persist even after in-situ reduction in the methanation reactor.

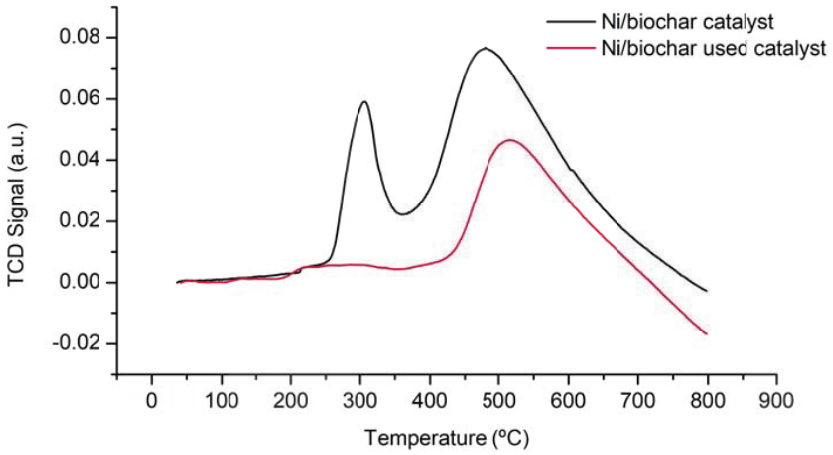

Figure 5: H2-TPR profiles of fresh and used Ni/biochar catalysts.

https://doi.org/10.52202/077185-0199

3.3 Kinetic model fitting and validation

Table 3 shows the parameters for the fitted kinetic equations from the experimental data related to the tests with 40 g of catalyst. The model is valid under the following operating conditions: 1 bar, 200 – 500 ºC, H_2:CO_2 ratio of 3.5 – 5.5, and GHSV 2000 - 10000 h^{-1}.

Table 3: Parameters of the kinetics for the CO_2 methanation.

Parameter	Units
$k_{1,0} = 5.645 \times 10^{-3}$	mol/(g_{cat} s Pa)
$k_{2,0} = 110.7 \times 10^{12}$	mol $Pa^{0.5}$/(g_{cat} s)
$E_{A,1} = 55045$	J/mol
$E_{A,2} = 226568$	J/mol
$K_{CO,0} = 2.16653 \times 10^{-7}$	1/Pa
$K_{H2,0} = 2.21403 \times 10^{-11}$	1/Pa
$K_{CH4,0} = 0.90785 \times 10^{-6}$	1/Pa
$K_{H2O,0} = 53.84 \times 10^{4}$	-

Figure 9 shows a comparison between the theoretical results of the fitted model and the experimental results. Dashed lines provide the discrepancy range of ±10%.

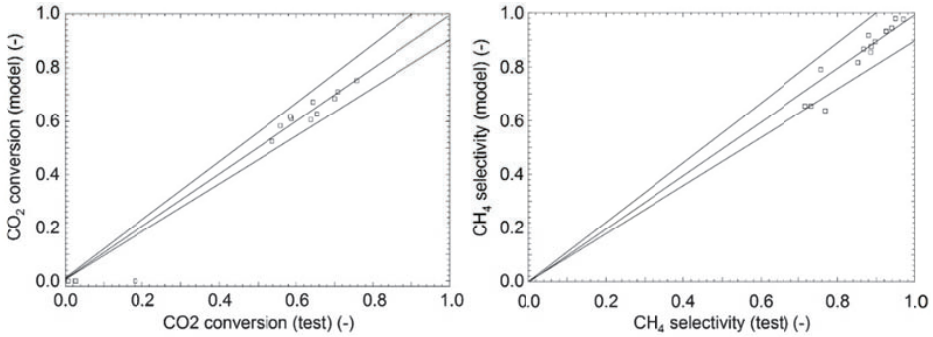

Figure 6: Comparison on CO_2 conversion and CH_4 selectivity between model and tests.

https://doi.org/10.52202/077185-0199

4. CONCLUSIONS

This paper has presented a preliminary study about the viability of using biochar as support for methanation catalysts. The samples of Ni-biochar catalyst were produced through batch pyrolysis of olive kernel and physically activated using steam at 750 °C. The Ni/biochar catalyst, prepared through wet impregnation, displayed a promising high surface area suitable for catalysis. However, the catalyst's incomplete reduction to its active metallic phase, evidenced by the persistence of residual NiO species even at a reduction temperature of 400 ºC after in-situ reduction in the methanation reactor and operation, highlights a notable aspect for further consideration and optimization in its application.

High conversion and selectivity has been obtained for the methanation process of CO_2 and H_2 in the fixed-beds containing 40 g of Ni-biochar catalyst. Nevertheless, the figures reached are below than that obtained for commercial catalysts with Al_2O_3 support. Notwithstanding, the results are promising and may serve as the starting point to improve the preparation process and to select the proper operation conditions with the aim of enhancing the performance of the biochar-based catalysts.

Finally, a kinetic model implemented in Aspen Plus has been adjusted and validated to potentially be used in integrated application models based in power to gas concepts. The kinetic model developed provides a good agreement with experimental test, valid for 1 bar, 200 – 500 ºC, H_2:CO_2 ratio of 3.5 – 5.5, and GHSV 2000 - 10000 h^{-1}. Further research will be done to improve the prediction at low conversion rates.

REFERENCES

Antoniak-Jurak, K., Kowalik, P., Konkol, M., Próchniak, W., Bicki, R., Raróg-Pilecka, W., Kuśtrowski, P., Ryczkowski, J., 2016. Sulfur tolerant Co-Mo-K catalysts supported on carbon materials for sour gas shift process - Effect of support modification. Fuel Processing Technology 144, 305–311. https://doi.org/10.1016/j.fuproc.2016.01.014

Antoniak-Jurak, K., Kowalik, P., Próchniak, W., Raróg-Pilecka, W., Kütrowski, P., Ryczkowski, J., 2015. Sour gas shift process over sulfided Co-Mo-K catalysts supported on carbon material - Support characterization and catalytic activity of catalysts. Fuel Processing Technology 138, 305–313. https://doi.org/10.1016/j.fuproc.2015.05.029

Avagyan, A.B., 2020. A Modified System of Nonlinear Fractional-Order Differential Equations in the Study of the Dynamics of Marital Relationships and their Behavioural Features. Athens J Sci 8, 57–80. https://doi.org/10.30958/ajs.8-1-4

Cam, L.M., Ha, N.T.T., Khu, L. Van, Ha, N.N., Brown, T.C., 2019. Carbon Dioxide Methanation over Nickel Catalysts Supported on Activated Carbon at Low Temperature. Aust J Chem 72, 969–977. https://doi.org/10.1071/CH19355

Di Stasi, C., Renda, S., Greco, G., González, B., Palma, V., Manyà, J.J., 2021. Wheat-straw-derived activated biochar as a renewable support of ni-ceo2 catalysts for co2 methanation. Sustainability (Switzerland) 13, 8939. https://doi.org/10.3390/su13168939

Dudek, M., Świechowski, K., Manczarski, P., Koziel, J.A., Białowiec, A., 2019. The effect of biochar addition on the biogas production kinetics from the anaerobic digestion of brewers' spent grain. Energies (Basel) 12, 1518. https://doi.org/10.3390/en12081518

Feng, Y., Yang, W., Chu, W., 2016. Effect of Ca modification on the catalytic performance of Ni/AC for CO_2 methanation. Integrated Ferroelectrics 172, 40–48. https://doi.org/10.1080/10584587.2016.1175333

Kumar, A., Sinha, A.S.K., 2020. Hydrogen production from acetic acid steam reforming over nickel-based catalyst synthesized via MOF process. Int J Hydrogen Energy 45, 24397–24411. https://doi.org/10.1016/j.ijhydene.2020.06.040

Luo, J., Chen, D., Yue, X., Feng, Y., Huang, Z., 2021. Study on syngas methanation over municipal solid waste char supported Ni catalyst. Fuel 303, 121222. https://doi.org/10.1016/j.fuel.2021.121222

https://doi.org/10.52202/077185-0199

Manyà, J.J., 2012. Pyrolysis for biochar purposes: A review to establish current knowledge gaps and research needs. Environ Sci Technol 46, 7939–7954. https://doi.org/10.1021/es301029g

Mei, Z., Chen, D., Feng, Y., Xin, Q., Yin, L., Qian, K., Hu, Y., 2023. Syngas methanation with municipal solid waste char supported Ni catalyst: Choice of key parameters and catalyst's response. Int J Hydrogen Energy 48, 10566–10578. https://doi.org/10.1016/j.ijhydene.2022.12.112

Paviotti, M.A., Faroldi, B.M., Cornaglia, L.M., 2021. Ni-based catalyst over rice husk-derived silica for the CO_2 methanation reaction: Effect of Ru addition. J Environ Chem Eng 9, 105173. https://doi.org/10.1016/j.jece.2021.105173

Petersen, E.M., Rao, R.G., Vance, B.C., Tessonnier, J.P., 2021. SiO2/SiC supports with tailored thermal conductivity to reveal the effect of surface temperature on Ru-catalyzed CO_2 methanation. Appl Catal B 286, 119904. https://doi.org/10.1016/j.apcatb.2021.119904

Renda, S., Di Stasi, C., Manyà, J.J., Palma, V., 2021. Biochar as support in catalytic CO_2 methanation: Enhancing effect of CeO_2 addition. Journal of CO_2 Utilization 53, 101740. https://doi.org/10.1016/j.jcou.2021.101740

Swalus, C., Jacquemin, M., Poleunis, C., Bertrand, P., Ruiz, P., 2012. CO_2 methanation on Rh/γ-Al_2O_3 catalyst at low temperature: "In situ" supply of hydrogen by Ni/activated carbon catalyst. Appl Catal B 125, 41–50. https://doi.org/10.1016/j.apcatb.2012.05.019

Vassiliadis, V.S., Conejeros, R., 2008. Powell Method, in: Encyclopedia of Optimization. pp. 3012–3013.

Wang, L., Luo, Q., Zhang, W., Yang, J., 2014. Transition metal atom embedded graphene for capturing CO: A first-principles study. Int J Hydrogen Energy 39, 20190–20196. https://doi.org/10.1016/j.ijhydene.2014.10.034

Wang, W., Duong-Viet, C., Ba, H., Baaziz, W., Tuci, G., Caporali, S., Nguyen-Dinh, L., Ersen, O., Giambastiani, G., Pham-Huu, C., 2019. Nickel Nanoparticles Decorated Nitrogen-Doped Carbon Nanotubes (Ni/N-CNT); A Robust Catalyst for the Efficient and Selective CO_2 Methanation. ACS Appl Energy Mater 2, 1111–1120. https://doi.org/10.1021/acsaem.8b01681

Xu, J., Froment, G., 1989. Methane Steam Reforming, Methanation and Water-Gas Shift: 1. Intrinsic Kinetics. AlChE Journal 35, 88–96.

Younas, M., Sethupathi, S., Kong, L.L., Mohamed, A.R., 2018. CO_2 methanation over Ni and Rh based catalysts: Process optimization at moderate temperature. Int J Energy Res 42, 3289–3302. https://doi.org/10.1002/er.4082

Yue, X., Chen, D., Luo, J., Huang, Z., Hong, L., Hu, Y., 2021. Direct synthesis of methane-rich gas from reed biomass pyrolysis volatiles over its biochar-supported Ni catalysts. Biomass Bioenergy 154, 106250. https://doi.org/10.1016/j.biombioe.2021.106250

ACKNOWLEDGMENT

This work is Part of the following R&D projects: PID2021-126164OB-I00, funded by MCIN/ AEI/10.13039/501100011033/ and by the "ERDF A way of making Europe"; SURFOLY project G.A. n.2014, Call 2020 Section 1 Farming IA, founded by the PRIMA program supported by the European Union; PRIN 2020 n. 2020AA9N4M_004 PE8 and the ECS00000041 - VITALITY, funded by the European Union - NextGenerationEU under the Italian Ministry of University and Research (MUR) National Innovation Ecosystem grant. Authors would like to acknowledge the use of Servicio General de Apoyo a la Investigación-SAI (Universidad de Zaragoza) and appreciate the help of J.A. Pastor and S. Arnau in setting up the experimental facility. This publication is supported by RYC2022-038283-I, funded by MCIN/ AEI/ 10.13039/ 501100011033 and the European Social Fund Plus (FSE+). C.B. also thanks the support received from the Investigo Program funding by the "European Union NextGenerationEU/PRTR".

 https://doi.org/10.52202/077185-0199